Stereotypic expansion of $T_{regulatory}$ and Th_{17} cells during infancy is disrupted by HIV exposure and gut epithelial damage.

Sonwabile Dzanibe[1*], Katie Lennard[2], Agano Kiravu[1], Melanie S.S. Seabrook[1,3], Berenice Alinde[1], Susan P. Holmes[4], Catherine A. Blish[5,6], Heather B. Jaspan[1,7] and Clive M. Gray[1,8]*

1. Division of Immunology, Institute of Infectious Diseases and Molecular Medicine, University of Cape Town, South Africa.
2. Division of Computational Biology, Institute of Infectious Diseases and Molecular Medicine, University of Cape Town, South Africa.
3. Department of Immunology, University of Toronto, Toronto, Canada
4. Department of Statistic, Stanford University, Stanford, CA USA
5. Department of Medicine, School of Medicine, Stanford University, Stanford, CA USA
6. Chan Zuckerberg Biohub, San Francisco, CA
7. Seattle Children's Research Institute and Departments of Paediatrics and Global Health, University of Washington, Seattle.
8. Division of Molecular Biology and Human Genetics, Stellenbosch University, Cape Town, South Africa.

Keywords: HIV-exposed uninfected infants, immune development, and intestinal damage

Count: Abstract: 134 words Text: 28685 characters

*Corresponding authors:
Sonwabile Dzanibe
Email: sonwabile.dzanibe@uct.ac.za

Clive M. Gray
Email: cgray@sun.ac.za

Conflict of interest statement: The authors have declared that no conflict of interest exists.

Summary

Few studies have investigated immune cell ontogeny throughout the period of increased vulnerability to infections in early life. Here, we evaluated the dynamics of two critical T cell populations, regulatory T (Treg) cells and Th17 cells, over the first 9 months of life. We observed that Treg and Th17 cells developed in a synchronous fashion. Infants exposed to HIV *in utero* (iHEU), who are more likely to develop infections, had a lower frequency of Tregs at birth and 36 weeks compared to HIV unexposed infants. This increased Th17/Treg ratio in iHEU was associated with impaired gut integrity at birth. These findings suggest that gut damage disrupts the Th17/Treg ratio during infant immune development, likely by attracting Treg cells to regulate inflammation occurring in the gut, so revealing an immune-gut nexus influenced by HIV exposure.

Introduction

Early infancy has the highest risk of mortality in children under 5 years, and with over 45% of these deaths occurring in the first month of life (Liu *et al.*, 2016). Neonates are more likely to succumb to infections compared to adults, largely due to their cellular immune system being less effective at protecting against invading pathogens (Dowling and Levy, 2014). Although the foetal immune system has matured by 15 weeks' gestation, foetal immunity exhibits heightened tolerogenic activity, Th2/Th17 polarisation bias, and lacks antigen experience which can result in blunted cellular immunity to pathogenic insults in early perinatal life (Mold *et al.*, 2010; Kollmann *et al.*, 2012; Ivarsson *et al.*, 2013; Kraft *et al.*, 2013). Following delivery, the neonatal immune system has to abruptly undergo adaptations to cope with extrauterine pathogens whilst developing tolerance to oral antigens and commensal microbes. Since postnatal immune interactions determine risk to subsequent infections and immune-related disease (Gensollen *et al.*, 2016; Torow and Hornef, 2017), understanding longitudinal ontogeny and factors that may disrupt development of the immune system are of critical importance in designing novel treatments and vaccine strategies to combat the high burden of disease in neonates.

$CD4^+$ helper T cells influence immunological responses to antigens either by promoting inflammation or establishing tolerance. T cell adaptive immunity among infants tends to exhibit weak Th1 polarization capacity (Kollmann *et al.*, 2012) and thus the homeostatic balance and interplay between Th17 and Treg cells during an inflammatory response is key to controlling infection while limiting immunopathology (Noack and Miossec, 2014). The ontogeny of these immune cells early in life is therefore crucial in establishing balanced immune responses towards pathogens, commensals and autoantigens. There are, however, limited studies reporting on the longitudinal development of Th17 and Treg cells, hence impeding potential corrective intervention strategies to ensure optimal protective immunity so being able to reduce the burden of infectious disease early in life.

There is a growing population of infants born to women living with HIV globally (Slogrove *et al.*, 2020), and although prenatal antiretroviral (ARV) treatment has reduced mother to child HIV transmission, HIV-exposed uninfected infants (iHEU) experience 60-70% higher mortality risk compared to their HIV-unexposed uninfected (iHUU) counterparts (Brennan *et al.*, 2016). Infectious diseases are the most likely cause of iHEU mortality, owing to higher rates of gastrointestinal and respiratory tract infections compared to iHUU (Cohen *et al.*, 2016; Slogrove *et al.*, 2016; Brennan *et al.*, 2019). It is possible that maternal HIV infection

can influence the Th17 and Treg immune balance in these children at birth and upset the trajectory of inflammatory versus tolerogenic immune cell ontogeny during early life. Thus, understanding the balance between immune inflammation and regulation in iHEU may also shed light on immune disturbances during infancy in general, and would also lay a foundation for providing more informed health-improving treatments for these vulnerable children.

Therefore, we aimed to define the ontogeny and relationship between Th17 and Treg cells in the first 9 months of life and examine how HIV/ARV exposure could impact the trajectory of these immune subsets. Here we show that the most dramatic change in the immune system occurs during the early period postpartum. Our data reveal that HIV/ARV exposure perturbs immune homeostatic and/or regulatory balance early in life, likely as a consequence of impaired epithelial gut integrity in iHEU compared to iHUU.

Results

Stereotypic expansion of Th17 and Treg cells from birth to 36 weeks

There is a paucity of data describing the ontogeny of Th17 and Treg cells throughout the first few months of life, with most studies comparing cord blood with infant and adult peripheral blood (Dirix, Vermeulen and Mascart, 2013; Collier *et al.*, 2015; Olin *et al.*, 2018). To describe the ontological changes occurring during infancy, we compared matched infant peripheral blood samples collected at birth, 7, 15 and 36 weeks of age from 16 healthy, term, breastfed infants. Thus, a total of sixty-four matching infant blood samples were analyzed by flow cytometry (FC) to determine the proportion of $CD4^{+}CCR6^{+}CCR4^{+}CD161^{+}$Th17 (Cosmi *et al.*, 2008) and $CD4{+}CD25^{hi}CD127^{-}FoxP3^{+}$ Treg cells reported as the percentage of $CD4^{+}$ cells (Table S1 and Figure S1). The proportions of Th17 cells were lowest at birth and gradually increased with age, peaking at 15 weeks (Figure 1A). Treg cells shared a similar stereotypic change as Th17 cells, being lowest at birth and increasing with age, although by 7 weeks the levels stabilized, and a marginal decline was observed by 36 weeks (Figure 1B). The similar stereotypic changes of Th17 and Treg cells in the first 36 weeks of life was reflected in the significant correlation found between these two populations (Figure 1C). Knowing that Treg and Th17 cells exhibit high plasticity and in specific conditions have been shown to undergo trans-differentiation between the two CD4 subsets (Gagliani *et al.*, 2015; Sehrawat and Rouse, 2017), we examined whether the co-linearity of these cells was due to marker co-expression. Using uniform manifold approximation and projection (UMAP) analysis, Treg and Th17 markers were expressed on distinct subsets of cells (Figure 1D). Our data reveal that circulating Treg and Th17 cells show similar stereotypic changes during

infancy and that the parallel changes of Treg and Th17 cells are not due to a co-lineage of cells but are distinct populations.

Cord blood and birth peripheral blood CD4 T cell populations are distinct.

Cord blood is frequently used as a proxy for infant blood in early life studies of the immune system for logistical reasons. Since the proportions of Th17 and Treg cells were lower in cord blood compared to birth blood (Figure 1A & B), we determined the similarity between cord blood and infant peripheral blood collected at birth. We used a multicolor FC panel (Table S1) to analyze $CD4^+$ phenotypes, in a limited set of 6 matching cord blood samples and peripheral blood collected within the first 12 hours of life. First, we performed multidimensional scaling (MDS) on the expression intensities of the cell markers included in the FC panel. $CD4^+$ cells from cord blood uniquely clustered away from birth blood samples (Figure 1E). To determine which cell markers distinguished cord and birth blood CD4 cells, we used generalised linear mixed model (GLMM) regression that calculates log-odds expression to identify markers predictive of either blood type (Seiler *et al.*, 2021) This approach showed significantly increased odds of birth peripheral blood $CD4^+$ cells expressing CCR7, CCR4, CCR6 and CD25 compared to cord blood (Figure 1F). Conversely, cord blood $CD4^+$ cells had increased odds of expressing FoxP3 compared to birth blood (Figure 1F). These data show that there are phenotypic differences of $CD4^+$ T cells between cord blood and birth blood. Despite the limited sample size, this suggests that cord blood should not be equated with birth blood and that rapid changes in circulating T cells occur within hours of delivery.

Identity of heterogenous CD4 clusters during infancy

Treg and Th17 cells are not necessarily a defined static population and varying phenotypes have been described that play specific immunological roles (Bystrom *et al.*, 2019; Matos *et al.*, 2021). To further define the heterogeneity of inflammatory versus regulatory CD4 cells during infancy in an unbiased manner; we used unsupervised Flow Self-Organizing Maps (FlowSOM) and hierarchical clustering to identify unique CD4 clusters of cells. Using this approach, we identified 9 $CD4^+$ T cell clusters. Figures 2A & B show delineation of the $CD4^+$ populations by the expression of cell surface markers and cell cluster relatedness is displayed using hierarchal clustering dendrograms and UMAP mapping. We identified two clusters of Treg cells, a small population of $CCR4^+$ Tregs and relatively larger population of $\alpha4\beta7^+$ Tregs. The CCR4+ Treg cluster co-expressed ectonucleotidase CD39, known to disrupt metabolic activity of activated and proliferating cells (Borsellino *et al.*, 2007), and the

inhibitory molecule, TIGIT, that prevents cognate interaction between antigen presenting cells and T helper cells (Joller *et al.*, 2014), suggesting that the $CCR4^+$ Treg cluster was a highly suppressive Treg population (Figure 2A). The 7-fold larger population of $\alpha4\beta7^+$ Tregs co-expressed $CCR7^+$, characteristic of gut trafficking lymphocytes (Figure 2A). Both these cell clusters were distinct from the 7 other CD4+ populations and showed a close relationship on the UMAP (Figure 2B). The trajectory and ontology of the FoxP3-expressing CD4 clusters showed differing levels of expansion after birth (Figures 2C & D). These cells increased following birth and remained relatively stable at later time points although by 36 weeks, the proportion of $CCR4^+$ Treg cluster decreased (Figure 2D). We also identified a Th17 cluster ($CCR6^+CCR4^+CD161^+$) that increased with advancing infant age and a cluster denoted as Th1/17 $\alpha4\beta7^+$ ($CCR6^+CCR4^-CD161^+$) was identified that gradually increased with infant age and peaked at 15 weeks (Figure 2C & D).

In addition to the Treg and Th17 cell clusters, we also identified $CD4^+$ clusters that expanded following birth, including Th2 ($CCR6^-CCR4^+$), Treg-like ($CD39^+CD25^+CCR6^+TIGIT^+\alpha4\beta7^+$) and a miscellaneous cluster that did not express any of the markers analysed (Figure 2C and D). A naïve-like cluster accounting for >80% of the CD4 cells at birth, significantly reduced at later time points, presumably as the other antigen-experienced cells expanded (Figure 2C). A similar $CD4^+$ cluster expressing $CD127^+$ $CCR7^+$ was observed that remained relatively stable from birth up to 36 weeks. Collectively, these findings show an expansion of differentiated $CD4^+$ T cell subsets with age compared to the decreasing frequency of naïve cells after delivery (Collier *et al.*, 2015). The most dramatic changes were observed to occur in the first 7 weeks of life, a period of immune plasticity as the adaptive immune system is likely shaped by environmental antigens postpartum (Gensollen *et al.*, 2016; Torow and Hornef, 2017).

Disrupted Th17-Treg ratio in iHEU

We next parsed out differences between $CD4^+$ clusters in iHEU from iHUU, as it is known that there is a more activated threshold of pro-inflammatory cytokine production from innate immune cells (Reikie *et al.*, 2014) and skewed adaptive immunity towards activated and exhausted cells in iHEU (Rich *et al.*, 1997; Clerici *et al.*, 2000; Rainwater-Lovett *et al.*, 2014). To assess whether these known alterations might be related to the Th17-Treg ratio, we compared the phenotype of $CD4^+$ cells of the 16 healthy infants (iHUU) with that of 20 iHEU. MDS of marker expression revealed distinct clustering of $CD4^+$ T cell marker expression between iHEU vs iHUU, regardless of age (Figure 3A). The observed differences

were driven by significantly higher odds of Foxp3 and CD161 expression in iHUU compared to iHEU, which persisted until 36 weeks of age (Figure 3B). By 36 weeks, log-odds expression of α4β7 was also dependent on HIV exposure, being higher in iHEU compared to iHUU (Figure 3B). These findings show that $CD4^+$ T cells of iHEU can be distinguished from that of iHUU primarily by higher expression of Foxp3 and CD161, which are Treg and Th17 discriminatory markers, respectively. We next performed differential abundance testing to assess whether HIV exposure alters the proportion of $CD4^+$ cell clusters defined in Figure 2A. Compared to iHUU, iHEU had significantly higher proportions of $\alpha4\beta7^+$ Th1/17 cluster at birth (Figure 3C). The minor, more highly suppressive $CCR4^+$ Treg cluster was lower at birth in iHEU compared to iHUU, albeit not statistically significant after adjusting for multiple comparisons (Figure 3C). Similarly, at 36 weeks, the gut homing $\alpha4\beta7^+$ Treg cluster was lower in iHEU compared to iHUU (Figure 3C). No differences were observed in the $CD4^+$ clusters between iHEU and iHUU at week 7 and 15 (data no shown).

When we assessed the proportion of Th17 and Treg cells using our manual gating approach, we found no significant differences in the proportions of Th17 cells between iHEU and iHUU (Figure S2A). However, iHEU had significantly lower proportions of Treg cells at birth (p=0.017) and at week 36 (p=0.012; Figure S2B). This resulted in a higher Th17-Treg ratio at birth and significantly so at 36 weeks (p=0.039) (Figure 3D). Overall, our data reveal that although circulating Th17 and Treg cells show similar stereotypic changes during infancy, iHEU have depressed frequencies of Treg cells accounting for the observed Th17-Treg imbalance at birth.

Treg and Th17 proportions associate with iFABP and gut-tropic chemokines and cytokines

Previous reports of intestinal damage leading to inflammation in iHEU (Prendergast *et al.*, 2017) led us to investigate the relationship between our different phenotypic clusters of cells with intestinal fatty-acid binding protein (iFABP) plasma concentrations. iFABP concentrations are elevated when there is impaired gut epithelial integrity leading to microbial translocation and gut inflammation (Wells *et al.*, 2017). Indeed, infant plasma concentrations of iFABP at birth were significantly higher in iHEU compared to iHUU (Figure 4A). By 36 weeks of life, no differences in iFABP concentrations were observed between iHEU and iHUU (Figure 4A), nor at weeks 7 and 15 (Figure S4A). We measured the concentration of inflammatory and regulatory chemokines and cytokines at birth and 36 weeks. Of the 10 analytes measured (Figures 4B & S3B), CCL17 was significantly higher in iHEU compared to iHUU at birth (Figure 4B). The regulatory cytokine, IL-27, involved in

epithelial restitution (Diegelmann *et al.*, 2012) was observed to be higher in iHEU, albeit not statistically significant after correcting for multiple comparisons (Figure 4B).

To integrate the multimodal cellular and protein data, we used generalized canonical regression to calculate RV coefficients of the latent variables determined by sparse partial least squares (sPLS). Using this approach, we assembled cluster image maps showing the association between $CD4^+$ clusters and plasma analytes (Figure 4C & F). At birth the Treg clusters shared a similar association with the measured analytes and were in stark contrast to Th17 and $CD127^+CCR6^+CCR7^+$ clusters (Figure 4C). Treg cluster frequency correlated inversely with iFABP, CCL17 and CCL20 concentrations, while positively with Th17 cluster frequency. Since iFABP and CCL17 were higher in iHEU and inversely associated with the population of Treg clusters, we postulate that these cells could be moving out of circulation and trafficking to the gut via CCL17 to mitigate epithelial damage and/or inflammation. Furthermore, using sPLS discriminant analysis (PLS-DA), we were able to determine the weighted score of each variable to predict HIV exposure: CCL17, IL27, $CCR4^+$ Tregs, $CD127^+CCR7^+$ T cells and iFABP were the strongest predictors of HIV exposure at birth with a classification error of 35% using latent variable-1 (LV-1) loadings (Figure 4D). ROC analysis using LV-1 loadings showed good discrimination between iHEU and iHUU with a highly significant (p=0.004) AUC of 0.85 (Figure 4E).

Although no differences in chemokine and cytokine concentrations were observed at 36 weeks (Figure 4B and S4B), there were correlations between these analytes and CD4+ T cell clusters that were similar to those found at birth (Figure 4F). Treg clusters (and the Th2 cluster) were positively correlated with IL27 and inversely correlated to iFABP, whereas $CD127^+CCR6^+CCR7^+$ and $\alpha4\beta7^+$ Th1/17 were inversely correlated to IL27 and positively to iFABP (Figure 4F). The strongest predictors of HIV exposure at 36 weeks were $\alpha4\beta7^+$ Treg and $\alpha4\beta7^+$ Th1/17 cell cluster together with IL17 and IL10, although having a higher classification error of 51% and LV-1 AUC=0.88 (Figures 4G & H). We further accessed the transcriptomic profile of Treg cells sorted into $\alpha4\beta7^+$ and $\alpha4\beta7^-$ populations (Figure S4A) at birth (n=4) and 15 weeks (n=5). According to PERMANOVA analysis considering HIV exposure, age and RNA integrity, HIV exposure explained 14% variance (p=0.047) of the $\alpha4\beta7^+$ Treg transcriptomic data set, while neither infant age nor RNA integrity were significant explanatory variables (Figure S4B). However, due to the small sample size we could not detect significant differentially expressed genes after adjusting for multiple comparisons (Data not shown). Collectively, these findings suggest that the perturbed Th17-

Treg ratio in iHEU could be related to intestinal epithelial gut damage or related to dysregulation of gut homeostatic balance, potentially by altered gut microbiota (Bender *et al.*, 2016).

Discussion

This study demonstrates the intricate homeostatic balance of $CD4^+$ T cell subsets during infancy that is necessary for appropriate responses to neoantigens, including pathogens, non-inherited maternal antigens, gut commensals and autoantigens. Although serving opposite roles during an inflammatory response, Th17 and Treg cells share similar features; both are dependent on TGF-β and IL-2 for their differentiation (Weaver *et al.*, 2006), exhibit specificity towards commensal-derived antigens and are abundant in the intestine to regulate homeostasis between the immune system and commensal microbes (Shen *et al.*, 2014). Overall, we observed a synchronous expansion of both Treg and Th17 cells early in life of healthy infants consistent with other reported studies (Black *et al.*, 2012; Collier *et al.*, 2015; Hayakawa *et al.*, 2017). The greatest increase observed was within the first 7 weeks of life suggesting a period of drastic changes as the infants are exposed to diverse environmental antigens and childhood vaccines and thus requires both the regulatory and inflammatory arms of the immune system.

We further demonstrate that HIV/ART exposure disrupts the emergent Th17-Treg homeostatic balance most likely via gut epithelial damage and potential homing of Treg cells to the gut at birth. It has previously been reported that iHEU, tend to display heightened immune activation compared to iHUU (Rich *et al.*, 1997; Clerici *et al.*, 2000; Rainwater-Lovett *et al.*, 2014), and we hypothesize from our data that this immune activation results from loss of balance between activation and tolerogenic signals. We provide evidence that the depressed Treg cells at birth in iHEU relative to iHUU are likely due to cells migrating out of circulation possibly to mitigate epithelial gut damage. This postulated model is based on a negative correlation between CCR4+ and α4β7+ Treg cells with plasma concentrations of iFABP and elevated levels of CCL17 and IL-27 in iHEU. Collectively, these events result in delayed peripheral ontogeny of these cells in iHEU, although by 7 weeks, iFABP and Treg cell levels are comparable between iHEU and iHUU. There is then a further progressive loss of Treg cells at 36 weeks of life, suggesting that the Th17-Treg balance may fluctuate in iHEU. Such fluctuating regulatory:inflammatory balance could in part be explained by the shifting gut microbiota profiles during weaning, thus impacting gut-immune axis pre-conditioned at birth (Bäckhed *et al.*, 2015; Al Nabhani *et al.*, 2019).

Our dataset reveals two different Treg populations that categorize infants by HIV-exposure at birth and week 36. As discussed above, events at birth are best explained by the trafficking of suppressive population of Treg cells for the reconstitution of gut epithelial damage in iHEU. Our integrated datasets could still distinguish the two groups of infants at 36 weeks of age where Treg $\alpha4\beta7^{+}$-IL10 and Th1/17 $\alpha4\beta7^{+}$-IL17 were predictive of iHUU and iHEU respectively. This evidence demonstrates long-lasting effects of *in utero* HIV and/or ARV exposure on the infants' Th17-Treg immune axis characteristic of the interplay of these immune cells in homeostatic maintenance in the gastrointestinal tract (Shen *et al.*, 2014; Omenetti and Pizarro, 2015).

This Th17-Treg imbalance is likely similar to the phenomenon that occurs in non-breastfed infants (Ardeshir *et al.*, 2014; Wood *et al.*, 2018). Th17-Treg imbalance has been reported in other infant diseases associated with gut damage such as neonatal necrotizing enterocolitis, where infants presenting with disease had lower frequencies of peripheral blood Treg cells (Pang *et al.*, 2018a, 2018b). These conditions are all associated with altered gut microbiota. Indeed, dysbiotic gut microbiota among iHEU relative to iHUU has been previously reported which could also explain altered inflammatory condition in the gut of iHEU associated with increased epithelial permeability (Bender *et al.*, 2016; Machiavelli *et al.*, 2019). iHEU were further observed to have significantly higher concentrations of IL-27 - a regulatory cytokine involved in wound healing including intestinal barrier protection (Diegelmann *et al.*, 2012; Yang *et al.*, 2017), and further supported that there was epithelial gut damage at birth. (Papasavvas *et al.*, 2011; Pilakka-Kanthikeel *et al.*, 2014). Whether this altered Th17/Treg ratio is associated with loss of tolerogenic signals as suggested by MHC inhibition from the transcriptomic data or an increased risk for disease among iHEU is unclear, but could in part explain the heightened risk of infections reported for iHEU compared to iHUU (Cohen *et al.*, 2016; Slogrove *et al.*, 2016; Brennan *et al.*, 2019).

The strength of our study lies in the cohort and matching of breastfed infants born to women living with HIV to those living without HIV from the same clinic and dwelling area. Further studies would need to investigate whether Treg cells have differing chemotactic activity between iHEU and iHUU. It is interesting to note that Jalbert et al (2019) reported higher frequencies of Treg cells in iHEU compared to iHUU (Jalbert *et al.*, 2019). However, this study used cord blood and compared iHUU from a U.S cohort with iHEU from South Africa. We showed that cord blood cellular constituents are distinct from birth peripheral blood and most likely does not reflect events in the newborn infant blood, agreeing with others (Olin *et*

al., 2018). It is also very important to have stringent measures of Treg cells, where minimal markers would be $CD4^+$ $CD25^{high}$ $Foxp3^+$ $CD127^-$ (Santegoets *et al.*, 2015).

The postnatal period is a critical window for priming and the maturation of the infants' immune system and its interaction with commensal microbes to facilitate homeostasis (Gensollen *et al.*, 2016; Torow and Hornef, 2017). Perturbations occurring during this "window of opportunity" alter ontogeny of immune development and likely associate with long-term immune-related diseases (Gensollen *et al.*, 2016; Olin *et al.*, 2018). This study shows that impact of HIV/ARV in the mother reveals a nexus between the gut and Th17:Treg homeostatic balance in the newborn infant.

Methods

Study participants

We conducted a longitudinal study on the effects of *in utero* HIV exposure on the phenotypic development of $CD4^+$ T lymphocytes during early infancy. Women were recruited to participate in the study within few hours following delivery as described (Tchakoute *et al.*, 2018). Women aged ≥18 years, who experienced no complications during pregnancy and provided signed informed consent for themselves and their respective infants were enrolled into the study approved by human research ethics committee of University of Cape Town (FWA1637; IRB0001938). Infants with gestational age <36 weeks and birth weight <2.4 kg were excluded from study analysis. Peripheral blood was collected from the infants at birth (<12 h), 7, 15 and 36 weeks of infant age. Among infants born to mothers living with HIV, absence of HIV transmission was confirmed by performing HIV DNA PCR test at 6 weeks of infant age. All infants received childhood vaccines according to the South African extended program of immunization schedule. A total of 36 infants; 20 iHEU and 16 iHUU were included in this analysis and followed over 36 weeks of life. To reduce potential confounding factors, samples were selected that showed no demographic difference between the two groups of infants (Table S2). All mothers elected to exclusively breastfeed at birth, although by 7 weeks only 52.8% were determined to be still exclusively breastfeeding (Table S2).

Whole blood collection

Blood was collected from the infants directly into sodium heparin tubes and transported to the laboratory for processing within 6h. BD FACS Lysing Solution (BD Biosciences, CA USA) was used for lysing of red blood cells and the fixation of the remaining peripheral blood mononuclear cells (PBMC) according to manufacturer's instructions. Fixed whole

blood cells were stored at -80^{o}C for 24 h in foetal calf serum with 10% DMSO and then cryopreserved at -180^{o}C until assayed using flow cytometry. Plasma samples were stored at -80^{o}C until used for serological analysis in this study.

Flow cytometry analysis

Immunophenotyping of CD4^{+} Th17 and Treg cells in infants was performed by staining thawed cells using a multi-colour antibody panel (Table S1). Lymphocytes were characterized by surface staining with antibodies specific to CD3, CD4 and CD8. To delineate Treg cells from the lymphocyte population, antibodies specific to surface makers CD127, CD25, CD39 and TIGIT together with transcription factor FoxP3 were used. Surface staining of CCR6, CCR4 and CD161 was used to define Th17 cells. Gut homing cells were defined using anti-$\alpha 4\beta 7$-surface staining. Immune cells migrating to the lymph nodes were characterized using CCR7 specific antibodies. Data acquisition was performed using BD LSR II and analysed with FlowJo software (version 10.5.3, Tree Star Inc., CA).

Quantification of intestinal fatty acid binding proteins using ELISA

Infant plasma samples collected at birth, 7, 15 and 36 weeks of age were used to measure the concentration of intestinal fatty-acid binding protein (IFABP) using a commercial ELISA kit (Elabscience). Test samples were diluted 1/400 in assay diluent and measured in duplicates according to manufacturer's instructions. An in-house high titre control plasma sample was included to determine intra-assay variation which had a coefficient of variation = 5.7%, indicating good intra-assay comparisons.

Quantification of chemokine and cytokine concentrations using multiplex immunoassay

A 10-plex immunoassay was designed to measure plasma concentrations of chemokines and cytokines in infant plasma samples collected at birth and 36 weeks of age. Using the multiplex immunoassay kit (R&D systems, Minneapolis, MN), we measured CCL17, CCL22, CXCL10 (IP10), CCL20 (MIP3A), CCL25, IL-6, IL-7, IL-17A, IL-10 and IL-27 concentrations according to manufacturer's instructions. Test samples were diluted 3:1 with assay diluent and signal intensity measured using Biorad-200 Luminex platform.

Transcriptomic analysis of Treg cells

We analysed the transcriptomic profile of sorted Treg cell populations (CD4^{+} CD25^{++} CD127^{-}) using PBMC samples collected from iHUU and iHEU at birth and 15 weeks of age of the same cohort. Two subsets of Treg cells were evaluated based on their surface

expression of the gut homing marker ($\alpha4\beta7$). Cells were purified using FACS Aria II (BD Science) into Fetal Calf Serum, washed and resuspended in RNAProtect (QAIGEN, Hilden, Germany). Extraction of RNA was carried out using RNeasy MicroPlus kit (QAIGEN, Hilden, Germany) according to manufacturer's instructions. Sample quality was assessed by Agilent RNA 6000 pico Reagent on Agilent 2100 Bioanalyzer (Agilent Technologies, Santa Clara, CA) and quantified by Qubit RNA HS assay (ThermoFisher, Waltham, MA). Samples were treated with DNAse prior to library preparation. Library preparation was performed with SMARTer Stranded Total RNA-Seq kit Pico Input v2 (Clontech Inc, Mountain View, CA) following manufacturer's instructions. Average final library size was 350 bp. Illumina 8-nt dual-indices were used for multiplexing. Samples were pooled and sequenced on Illumina HiSeq X sequencer for 150 bp read length in paired-end mode, with an output of 80 million reads per sample. Illumina reads were processed using the nf-core rnaseq pipeline v1.4.2 pipeline using GRCh37 genome as reference sequence (Ewels *et al.*, 2020). Briefly, reads were trimmed with Trim Galore, ribosomal RNA removed with SortMeRNA (Kopylova, Noé and Touzet, 2012), read alignment was performed using STAR (Dobin *et al.*, 2013), and mapped reads were summarized at gene level using the featureCounts function from the R package Rsubread (Liao, Smyth and Shi, 2019).

Statistical analysis

R software (version 3.5 R Core Team, Vienna, Austria) was used to test for statistical differences. The cell populations described in the study are reported as median percentages. iFABP concentrations were $\log_{10}$ transformed for statistical comparisons. Nominal variables were compared using χ^2 or Fisher exact test. Differences in cell frequencies between the two groups of infants were compared using the Mann-Whitney U test. Friedman's test was used to compare differences within a group over time. Chemokine and cytokines included in a multiplex immunoassay were compared using Mann-Whitney test and Bonferroni correction used to adjust for multiple comparisons.

Coordinates for multi-dimensional scaling for the markers expressed on $CD4^+$ cells were calculated using metaMDS function and PERMANOVA statistical differences performed using the adonis function from the vegan R package. GLMM analysis was performed using an open-source R package CytoGLMM as described in (Seiler *et al.*, 2021). Unsupervised cell population identification was performed using self-organizing map and hierarchal clustering as implemented in the FlowSOM and metaclustering R packages (Nowicka *et al.*, 2017). The mixomics R package was used to integrate the identified $CD4^+$ cell clusters with

the measured plasma analytes. RV coefficients were computed, and the latent variables determined by sparse partial least squares (sPLS). To determine the strongest predictors of HIV exposure at birth and week 36 we performed sPLS-DA and computed the loading plot and ROC plot of component 1 of all variables in our data set (Rohart *et al.*, 2017). p-value < 0.05 was considered statistically significant.

Acknowledgments

The authors would like to thank all the mothers and infants who volunteered to participate in this study and the dedicated work of the INFANT team. This study was supported by the South African Medical Research Council (SA-MRC) Self-Initiated Research Grant and NIH awards U01 AI131302 and R01 HD102050. SD is supported by the Claude Leon Fellowship.

Author contributions

The study was conceived and designed by SD, CAB, HBJ and CMG. SD, MSSS and AK designed flow cytometry and cell sorting experiments. BA and HBJ were responsible for participant enrolment, sample collection and processing. Data generation and acquisition was performed by SD and analysed by SD, KL, and SPH. SD drafted the original manuscript that was reviewed and edited by all authors.

Declaration of Interest

The authors declare no competing interests.

Figure legends

Figure 1 Stereotypic expansion of Th17 and Treg cells from birth to 36 weeks. A & B) Kinetic changes in the frequency of Th17 and Treg cells from birth up until 36 weeks of age. C) Spearman rank correlation between Th17 and Treg cells. D) UMAP analysis displaying Foxp3 and CD161 expression in $CD4^+$ cells distinguishing co-lineage of Treg cells and Th17 cells. E) Multidimensional scaling (MDS) showing dissimilarity of $CD4^+$ cells from cord and peripheral blood at birth. B) Generalized linear mixed model comparing CD4 marker expression between cord blood and peripheral blood at birth.

Figure 2 Identity of heterogenous CD4 clusters during infancy. A) Hierarchical clustering of $CD4^+$ cell clusters identified using FlowSOM. B) Dimensional reduction projecting the CD4 clusters on UMAP. C) Relative abundance of $CD4^+$ cell clusters at birth, 7, 15 and 36 weeks. D) Boxplot showing stereotypic changes in CD4 clusters with increasing infant age.

Figure 3 In utero HIV exposure disrupts Th17/Treg ratio during infancy A) Multidimensional scaling (MDS) showing dissimilarity of $CD4^+$ between HIV-exposed uninfected infants (iHEU) and HIV-unexposed uninfected infants (iHUU). B) Generalized linear mixed model comparing CD4 marker expression between iHEU and iHUU. C) Differential abundance of CD4 cell clusters in iHEU and iHUU at birth and week 36. D) Log2 Th17/Treg ratio.

Figure 4 Gut epithelial integrity and proinflammatory and regulatory milieu associated with Th17 and Treg cells. A) Comparing intestinal fatty acid binding protein (iFABP) concentration between HIV-unexposed uninfected infants (iHUU) and HIV-exposed uninfected infants (iHEU). B) Chemokine and cytokine concentrations in iHUU and iHEU at birth and 36 weeks. C) Cluster image map showing RV correlation of CD4 clusters with iFABP, chemokine and cytokine concentrations. D) Sparse PLS discriminant analysis (sPLS-DA) between HUU and HEU using CD4 clusters and chemokine data set E) ROC-curve analysis of LV-1 loadings at birth. F) Cluster image map of CD4 clusters and iFABP, chemokine and cytokine concentrations. G) sPLS-DA H) ROC-curve analysis of LV-1 loadings at week 36.

Supplementary information

Table legends

Table S1 Flow cytometry antibody panel used to surface and intracellular stain infant whole blood to characterize T cells.

Table S2 Demographic characteristic of HIV infected-exposed and HIV uninfected-unexposed mother-infant pairs.

Figure legends

Figure S1 Flow cytometry gating strategy to identify T regulatory and Th17 cells.

Figure S2 Ontological changes of CD4+ cells in HIV-exposed uninfected (HEU) and HIV-unexposed uninfected (HUU) infants. A) Th17 and B) Treg cells.

Figure S3 Plasma analytes measure in HIV-exposed uninfected infants (iHEU) and HIV-unexposed uninfected infants (iHUU). A) Comparisons of iFABP concentrations between iHEU and iHUU measured at 7 and 15 weeks. B) Chemokine and cytokine concentrations measured at birth and 36 weeks of age.

Figure S4 HIV exposure alters transcriptomic profile of gut homing Treg cells. A) Flow plot showing sorting of α4β7- and α4β7+ Treg cells. B) NMDS plots showing Bray Curtis distances between infant samples.

References

Ardeshir, A. *et al.* (2014) 'Breast-fed and bottle-fed infant rhesus macaques develop distinct gut microbiotas and immune systems', *Science Translational Medicine*, 6(252). doi: 10.1126/scitranslmed.3008791.

Bäckhed, F. *et al.* (2015) 'Dynamics and stabilization of the human gut microbiome during the first year of life', *Cell Host and Microbe*, 17(5), pp. 690–703. doi: 10.1016/j.chom.2015.04.004.

Bender, J. M. *et al.* (2016) 'Maternal HIV infection influences the microbiome of HIV-uninfected infants', *Science Translational Medicine*, 8(349), p. 349ra100.

Black, A. *et al.* (2012) 'Developmental regulation of Th17-cell capacity in human neonates', *European Journal of Immunology*, 42(2), pp. 311–319. doi: 10.1002/eji.201141847.

Borsellino, G. *et al.* (2007) 'Expression of ectonucleotidase CD39 by Foxp3+ Treg cells: hydrolysis of extracellular ATP and immune suppression', *Blood*, 110(4), pp. 1225–1232. doi: 10.1182/blood-2006-12-064527.The.

Brennan, A. T. *et al.* (2016) 'A meta-analysis assessing all-cause mortality in HIVexposed uninfected compared with HIV-unexposed uninfected infants and children', *Aids*, 30(15), pp. 2351–2360. doi: 10.1097/QAD.0000000000001211.

Brennan, A. T. *et al.* (2019) 'A meta-analysis assessing diarrhea and pneumonia in HIV-exposed uninfected compared to HIV-unexposed uninfected infants and children', *JAIDS Journal of Acquired Immune Deficiency Syndromes*, 82(1), pp. 1–8. doi: 10.1097/qai.0000000000002097.

Bystrom, J. *et al.* (2019) 'Functional and phenotypic heterogeneity of Th17 cells in health and disease', *European Journal of Clinical Investigation*, 49(1), pp. 1–13. doi: 10.1111/eci.13032.

Clerici, M. *et al.* (2000) 'T-lymphocyte maturation abnormalities in uninfected newborns and children with vertical exposure to HIV T-lymphocyte maturation abnormalities in uninfected newborns and children with vertical exposure to HIV', *Bloid*, 96, pp. 3866–3871.

Cohen, C. *et al.* (2016) 'Epidemiology of Acute Lower Respiratory Tract Infection in HIV-Exposed Uninfected Infants', *Pediatrics*, 137(4), p. e20153272.

Collier, F. M. *et al.* (2015) 'The ontogeny of naive and regulatory CD4+ T-cell subsets duing the first postnatal year: a cohort study', *Clinical and Translational Immunology*, 4(3), p. e34.

doi: 10.1038/cti.2015.2.

Cosmi, L. *et al.* (2008) 'Human interleukin 17-producing cells originate from a CD161 +CD4+ T cell precursor', *Journal of Experimental Medicine*, 205(8), pp. 1903–1916. doi: 10.1084/jem.20080397.

Diegelmann, J. *et al.* (2012) 'A novel role for interleukin-27 (IL-27) as mediator of intestinal epithelial barrier protection mediated via differential signal transducer and activator of transcription (STAT) protein signaling and induction of antibacterial and anti-inflammatory protei', *Journal of Biological Chemistry*, 287(1), pp. 286–298. doi: 10.1074/jbc.M111.294355.

Dirix, V., Vermeulen, F. and Mascart, F. (2013) 'Maturation of CD4+ regulatory T lymphocytes and of cytokine secretions in infants born prematurely', *Journal of Clinical Immunology*, 33(6), pp. 1126–1133. doi: 10.1007/s10875-013-9911-4.

Dobin, A. *et al.* (2013) 'STAR: Ultrafast universal RNA-seq aligner', *Bioinformatics*, 29(1), pp. 15–21. doi: 10.1093/bioinformatics/bts635.

Dowling, D. J. and Levy, O. (2014) 'Ontogeny of early life immunity', *Trends in Immunology*. Elsevier Ltd, 35(7), pp. 299–310. doi: 10.1016/j.it.2014.04.007.

Ewels, P. A. *et al.* (2020) 'The nf-core framework for community-curated bioinformatics pipelines', *Nature Biotechnology*, 38(3), pp. 276–278. doi: 10.1038/s41587-020-0439-x.

Gagliani, N. *et al.* (2015) 'Th17 cells transdifferentiate into regulatory T cells during resolution of inflammation.', *Nature*, 523(7559), pp. 221–5. doi: 10.1038/nature14452.

Gensollen, T. *et al.* (2016) 'How colonization by microbiota in early life shapes the immune system', *Science*, 352(6285), pp. 539–544. doi: 10.1126/science.aad9378.

Hayakawa, S. *et al.* (2017) 'Significant augmentation of regulatory T cell numbers occurs during the early neonatal period', *Clinical and Experimental Immunology*, 190(2), pp. 268–279. doi: 10.1111/cei.13008.

Ivarsson, M. A. *et al.* (2013) 'Differentiation and functional regulation of human fetal NK cells', *Journal of Clinical Investigation*, 123(9), pp. 3889–3901. doi: 10.1172/JCI68989.

Jalbert, E. *et al.* (2019) 'HIV-exposed uninfected infants have increased regulatory T cells that correlate with decreased T cell function', *Frontiers in Immunology*, 10(MAR), pp. 1–9. doi: 10.3389/fimmu.2019.00595.

Joller, N. *et al.* (2014) 'Treg cells expressing the co-inhibitory molecule TIGIT selectively inhibity pro-inflammatory Th1 and Th17 cell responses', *Immunity*, 40(4), pp. 569–581. doi: 10.1016/j.immuni.2014.02.012.Treg.

Kollmann, T. R. *et al.* (2012) 'Innate Immune Function by Toll-like Receptors: Distinct Responses in Newborns and the Elderly', *Immunity*. Elsevier Inc., 37(5), pp. 771–783. doi:

10.1016/j.immuni.2012.10.014.

Kopylova, E., Noé, L. and Touzet, H. (2012) 'SortMeRNA: Fast and accurate filtering of ribosomal RNAs in metatranscriptomic data', *Bioinformatics*, 28(24), pp. 3211–3217. doi: 10.1093/bioinformatics/bts611.

Kraft, J. D. *et al.* (2013) 'Neonatal macrophages express elevated levels of interleukin-27 that oppose immune responses', *Immunology*, 139(4), pp. 484–493. doi: 10.1111/imm.12095.

Liao, Y., Smyth, G. K. and Shi, W. (2019) 'The R package Rsubread is easier, faster, cheaper and better for alignment and quantification of RNA sequencing reads', *Nucleic Acids Research*. Oxford University Press, 47(8). doi: 10.1093/nar/gkz114.

Liu, L. *et al.* (2016) 'Global, regional, and national causes of under-5 mortality in 2000–15: an updated systematic analysis with implications for the Sustainable Development Goals', *The Lancet*. The Author(s). Published by Elsevier Ltd. This is an Open Access article under the CC BY license, 388(10063), pp. 3027–3035. doi: 10.1016/S0140-6736(16)31593-8.

Machiavelli, A. *et al.* (2019) 'The impact of in utero HIV exposure on gut microbiota, inflammation, and microbial translocation', *Gut Microbes*. Taylor & Francis, 10(5), pp. 599–614. doi: 10.1080/19490976.2018.1560768.

Matos, T. R. *et al.* (2021) 'Maturation and Phenotypic Heterogeneity of Human CD4+ Regulatory T Cells From Birth to Adulthood and After Allogeneic Stem Cell Transplantation', *Frontiers in Immunology*, 11(January), pp. 1–10. doi: 10.3389/fimmu.2020.570550.

Mold, J. E. *et al.* (2010) 'Fetal and Adult Hematopoietic Stem Cells Give Rise to Distinct T Cell Lineages in Humans', *Science*, 330(6011), pp. 1695–9.

Al Nabhani, Z. *et al.* (2019) 'A Weaning Reaction to Microbiota Is Required for Resistance to Immunopathologies in the Adult', *Immunity*, 50(5), pp. 1276-1288.e5. doi: 10.1016/j.immuni.2019.02.014.

Noack, M. and Miossec, P. (2014) 'Th17 and regulatory T cell balance in autoimmune and inflammatory diseases', *Autoimmunity Reviews*. Elsevier B.V., 13(6), pp. 668–677. doi: 10.1016/j.autrev.2013.12.004.

Nowicka, M. *et al.* (2017) 'CyTOF workflow: Differential discovery in high-throughput high-dimensional cytometry datasets', *F1000Research*, 6(748). doi: 10.12688/f1000research.11622.1.

Olin, A. *et al.* (2018) 'Stereotypic Immune System Development in Newborn Children', *Cell*. Elsevier Inc., 174(5), pp. 1277-1292.e14. doi: 10.1016/j.cell.2018.06.045.

Omenetti, S. and Pizarro, T. T. (2015) 'The Treg/Th17 axis: A dynamic balance regulated by the gut microbiome', *Frontiers in Immunology*, 6(DEC), pp. 1–8. doi:

10.3389/fimmu.2015.00639.

Pang, Y. *et al.* (2018a) 'Impairment of regulatory T cells in patients with neonatal necrotizing enterocolitis', *International Immunopharmacology*. Elsevier, 63(May), pp. 19–25. doi: 10.1016/j.intimp.2018.07.029.

Pang, Y. *et al.* (2018b) 'Monocyte activation and inflammation can exacerbate Treg/Th17 imbalance in infants with neonatal necrotizing enterocolitis', *International Immunopharmacology*. Elsevier, 59(April), pp. 354–360. doi: 10.1016/j.intimp.2018.04.026.

Papasavvas, E. *et al.* (2011) 'Increased microbial translocation in ≤180 days old perinatally human immunodeficiency virus-positive infants as compared with human immunodeficiency virus-exposed uninfected infants of similar age', *Pediatric Infectious Disease Journal*, 30(10), pp. 877–882. doi: 10.1097/INF.0b013e31821d141e.

Pilakka-Kanthikeel, S. *et al.* (2014) 'Immune activation is associated with increased gut microbial translocation in treatment-naive, HIV-infected children in a resource-limited setting', *Journal of Acquired Immune Deficiency Syndromes*, 66(1), pp. 16–24. doi: 10.1097/QAI.0000000000000096.

Prendergast, A. J. *et al.* (2017) 'Intestinal Damage and Inflammatory Biomarkers in Human Immunodeficiency Virus (HIV)-Exposed and HIV-Infected Zimbabwean Infants', *Journal of Infectious Diseases*, 216(6), pp. 651–661. doi: 10.1093/infdis/jix367.

Rainwater-Lovett, K. *et al.* (2014) 'Changes in Cellular Immune Activation and Memory T Cell Subsets in HIV-Infected Zambian Children Receiving HAART.', *Journal of acquired immune deficiency syndromes (1999)*, 67(5), pp. 455–462. doi: 10.1097/QAI.0000000000000342.

Reikie, B. A. *et al.* (2014) 'Altered innante immune development in HIV-exposed uninfected infants', *Journal of Acquired Immune Deficiency Syndriome*, 66(3), pp. 245–255. doi: 10.1097/QAI.0000000000000161.Altered.

Rich, K. C. *et al.* (1997) 'Function and phenotype of immature CD4+ lymphocytes in healthy infants and early lymphocyte activation in uninfected infants of human immunodeficiency virus-infected mothers.', *Clinical and diagnostic laboratory immunology*, 4(3), pp. 358–361.

Rohart, F. *et al.* (2017) 'mixOmics: An R package for 'omics feature selection and multiple data integration', *PLoS Computational Biology*, 13(11), pp. 1–19. doi: 10.1371/journal.pcbi.1005752.

Santegoets, S. J. A. M. *et al.* (2015) 'Monitoring regulatory T cells in clinical samples: consensus on an essential marker set and gating strategy for regulatory T cell analysis by flow cytometry', *Cancer Immunology, Immunotherapy*. Springer Berlin Heidelberg, 64(10), pp. 1271–1286. doi: 10.1007/s00262-015-1729-x.

637 Sehrawat, S. and Rouse, B. T. (2017) 'Interplay of regulatory T cell and Th17 cells during
638 infectious diseases in humans and animals', *Frontiers in Immunology*, 8(APR), pp. 1–14. doi:
639 10.3389/fimmu.2017.00341.
640 Seiler, C. *et al.* (2021) 'CytoGLMM: conditional differential analysis for flow and mass
641 cytometry experiments', *BMC Bioinformatics*. BioMed Central, 22(1), pp. 1–14. doi:
642 10.1186/s12859-021-04067-x.
643 Shen, X. *et al.* (2014) 'The balance of intestinal Foxp3+ regulatory T cells and Th17 cells and
644 its biological significance', *Expert Review of Clinical Immunology*, 10(3), pp. 353–362. doi:
645 10.1586/1744666X.2014.882232.
646 Slogrove, A. L. *et al.* (2016) 'Pattern of Infectious Morbidity in HIV-Exposed Uninfected
647 Infants and Children', *Frontiers in Immunology*, 7(164), pp. 1–8. doi:
648 10.3389/fimmu.2016.00164.
649 Slogrove, A. L. *et al.* (2020) 'Estimates of the global population of children who are HIV-
650 exposed and uninfected, 2000–18: a modelling study', *The Lancet Global Health*. The
651 Author(s). Published by Elsevier Ltd. This is an Open Access article under the CC BY-NC-
652 ND 4.0 license, 8(1), pp. e67–e75. doi: 10.1016/S2214-109X(19)30448-6.
653 Tchakoute, C. T. *et al.* (2018) 'Breastfeeding mitigates the effects of maternal HIV on infant
654 infectious morbidity in the Option B+ era', *AIDS (London, England)*, 32(16), pp. 2383–2391.
655 doi: 10.1097/QAD.0000000000001974.
656 Torow, N. and Hornef, M. W. (2017) 'The Neonatal Window of Opportunity: Setting the
657 Stage for Life-Long Host-Microbial Interaction and Immune Homeostasis', *The Journal of*
658 *Immunology*, 198(2), pp. 557–563. doi: 10.4049/jimmunol.1601253.
659 Weaver, C. T. *et al.* (2006) 'Th17: An Effector CD4 T Cell Lineage with Regulatory T Cell
660 Ties', *Immunity*, 24(6), pp. 677–688. doi: 10.1016/j.immuni.2006.06.002.
661 Wells, J. M. *et al.* (2017) 'Homeostasis of the gut barrier and potential biomarkers',
662 *American Journal of Physiology - Gastrointestinal and Liver Physiology*, 312(3), pp. G171–
663 G193. doi: 10.1152/ajpgi.00048.2015.
664 Wood, L. F. *et al.* (2018) 'Feeding-Related Gut Microbial Composition Associates with
665 Peripheral T-Cell Activation and Mucosal Gene Expression in African Infants', *Clinical*
666 *Infectious Diseases*, 67(8), pp. 1237–1246. doi: 10.1093/cid/ciy265.
667 Yang, B. *et al.* (2017) 'IL-27 Facilitates Skin Wound Healing through Induction of
668 Epidermal Proliferation and Host Defense', *Journal of Investigative Dermatology*, 137(5),
669 pp. 1166–1175. doi: 10.1016/j.jid.2017.01.010.
670

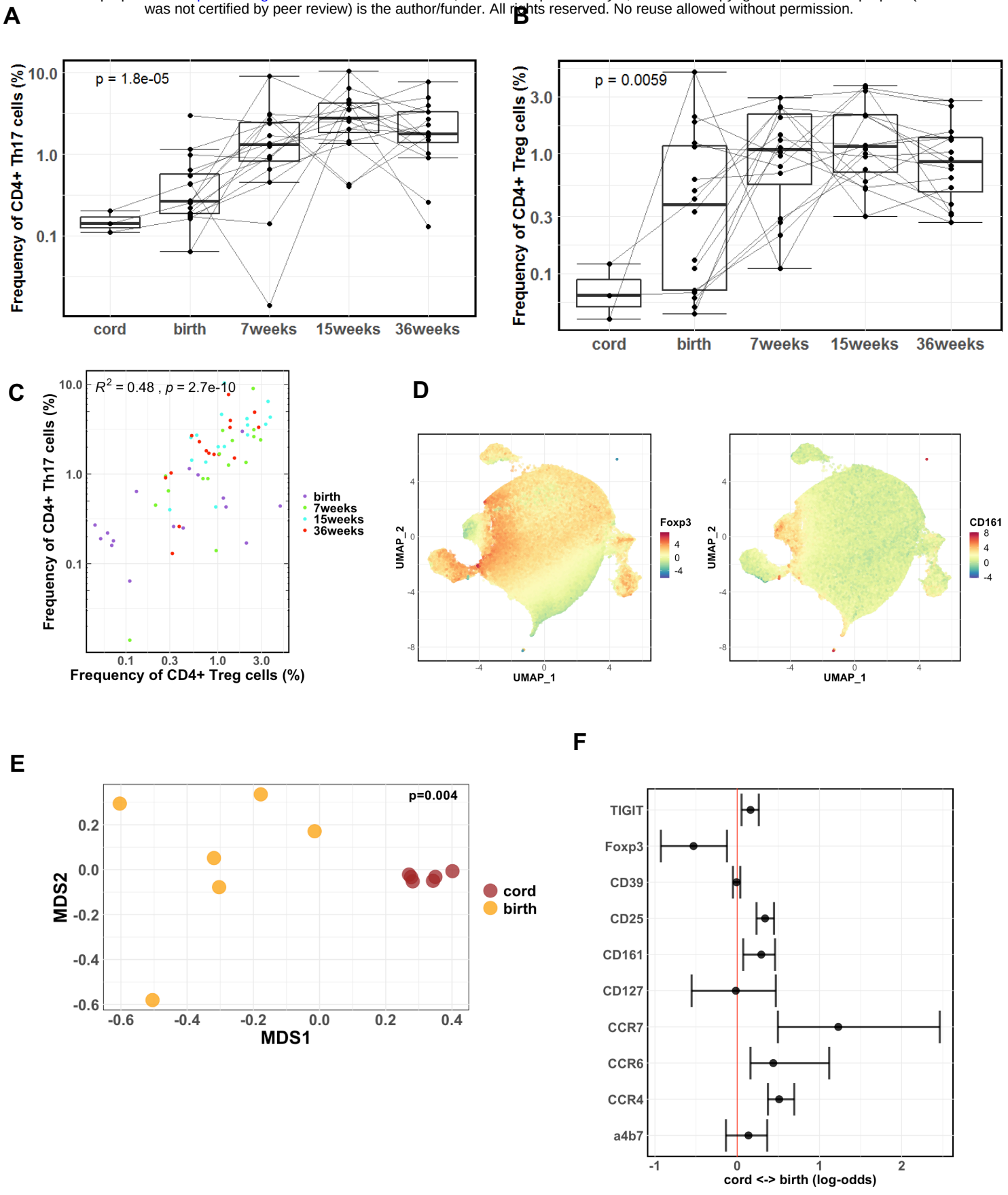

Figure 1 Stereotypic expansion of Th17 and Treg cells from birth to 36 weeks. A & B) Kinetic changes in the frequency of Th17 and Treg cells from birth up until 36 weeks of age. C) Spearman rank correlation between Th17 and Treg cells. D) UMAP analysis displaying Foxp3 and CD161 expression in $CD4^+$ cells distinguishing co-lineage of Treg cells and Th17 cells. E) Multidimensional scaling (MDS) showing dissimilarity of $CD4^+$ cells from cord and peripheral blood at birth. B) Generalized linear mixed model comparing CD4 marker expression between cord blood and peripheral blood at birth

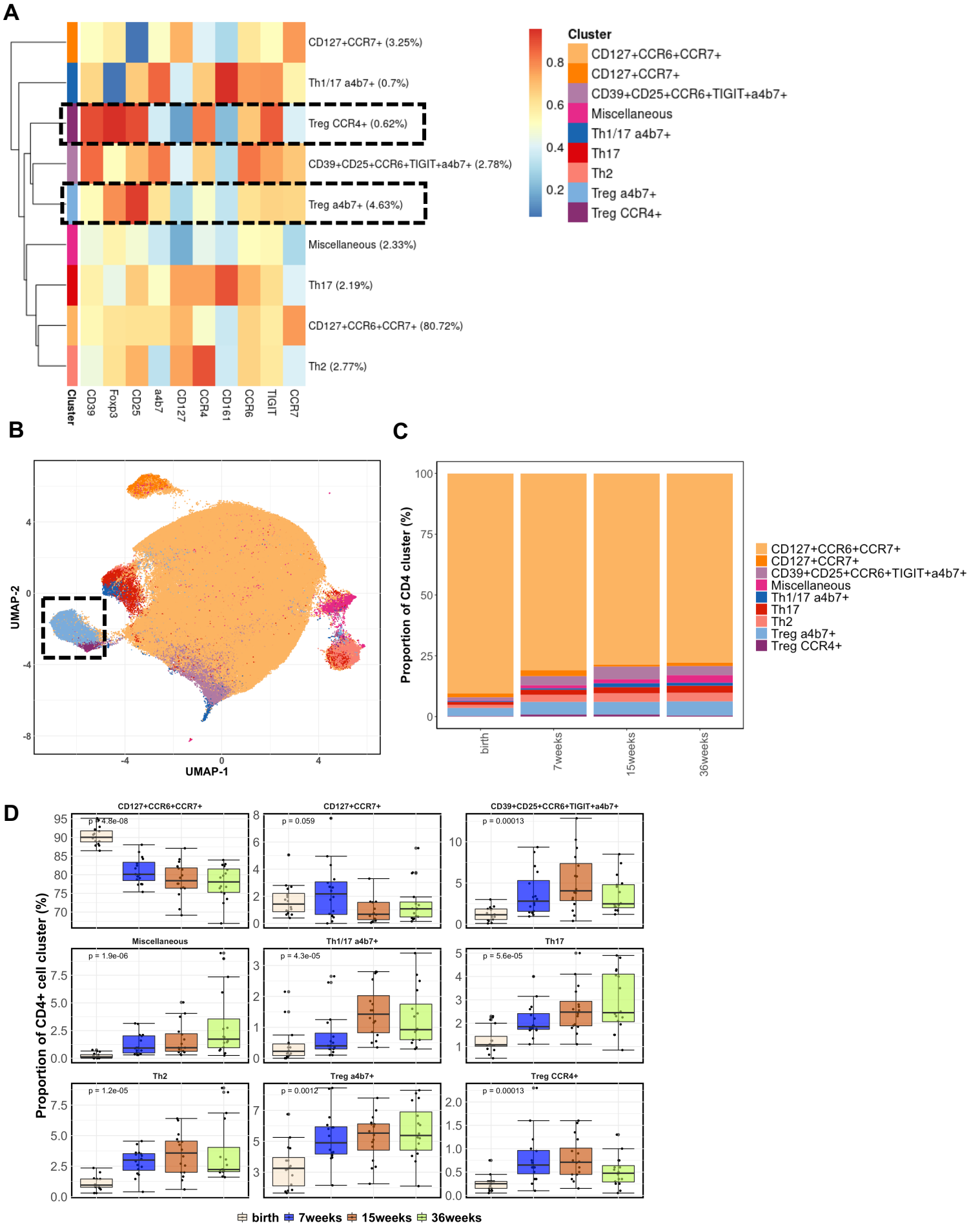

Figure 2 Identity of heterogenous CD4 clusters during infancy. A) Hierarchical clustering of CD4$^+$ cell clusters identified using FlowSOM. B) Dimensional reduction projecting the CD4 clusters on UMAP. C) Relative abundance of CD4$^+$ cell clusters at birth, 7, 15 and 36 weeks. D) Boxplot showing stereotypic changes in CD4 clusters with increasing infant age.

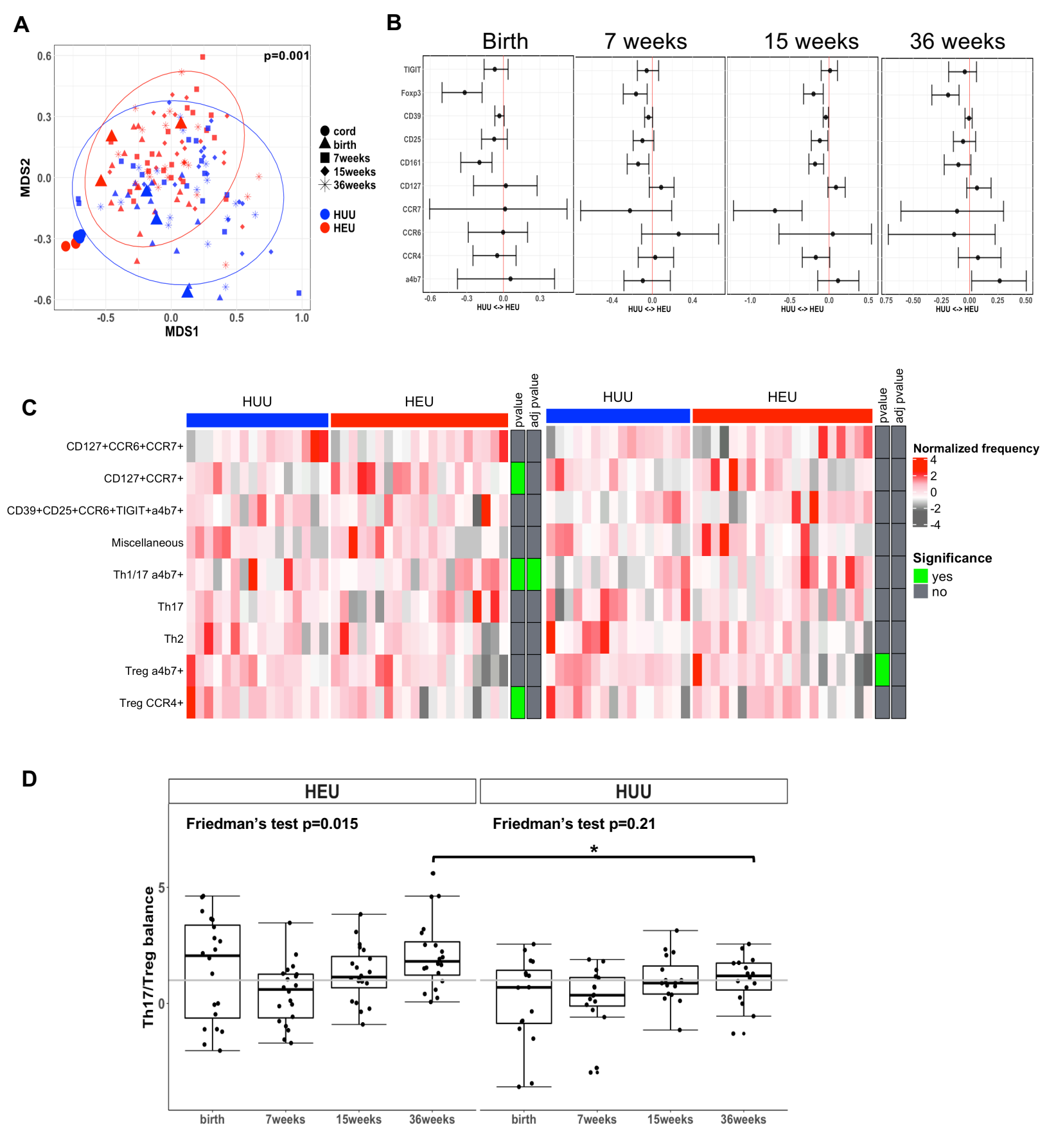

Figure 3 In utero HIV exposure disrupts Th17/Treg ratio during infancy A) Multidimensional scaling (MDS) showing dissimilarity of CD4⁺ between HIV-exposed uninfected infants (iHEU) and HIV-unexposed uninfected infants (iHUU). B) Generalized linear mixed model comparing CD4 marker expression between iHEU and iHUU. C) Differential abundance of CD4 cell clusters in iHEU and iHUU at birth and week 36. D) Log2 Th17/Treg ratio.

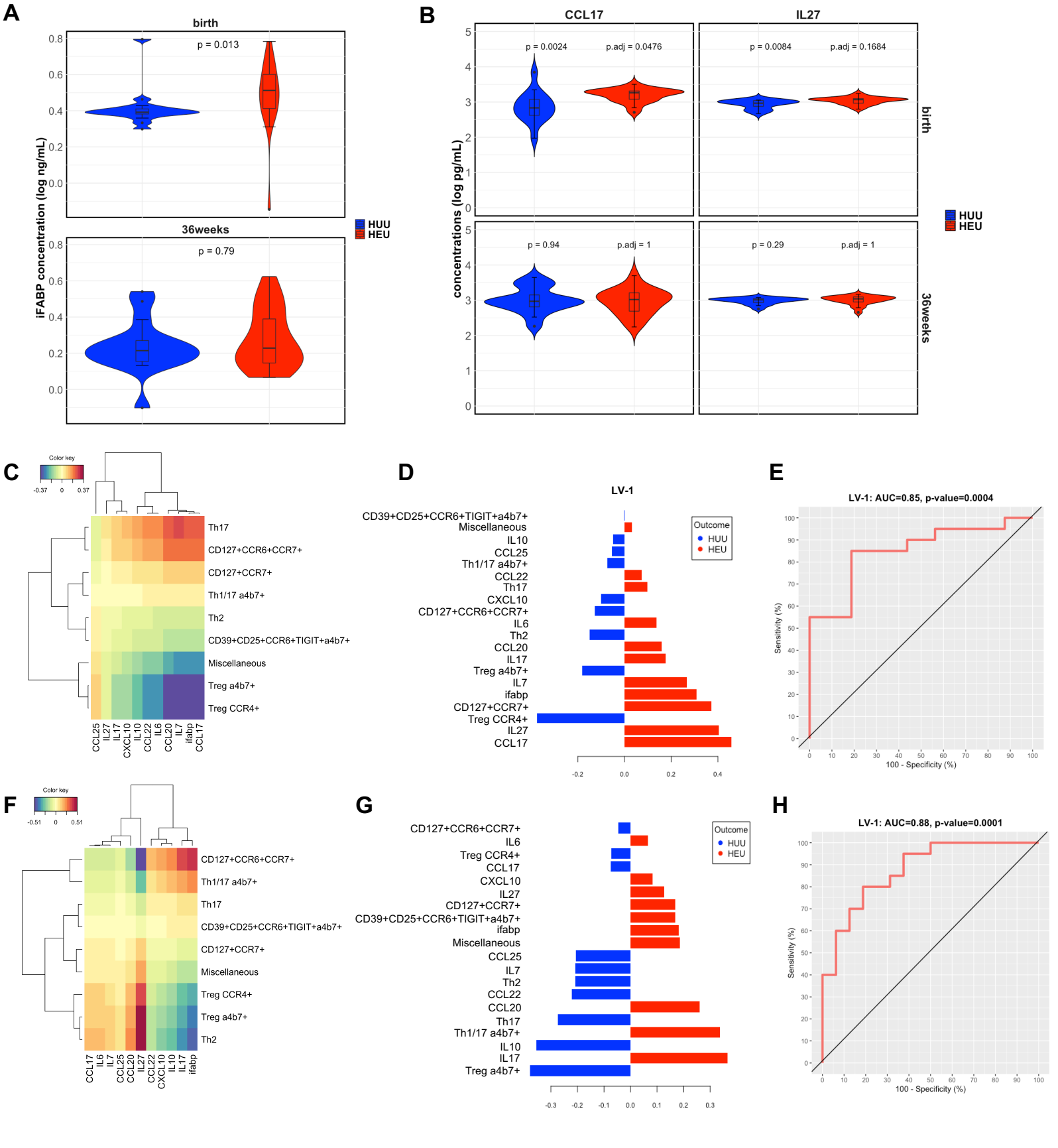

Figure 4 Gut epithelial integrity and proinflammatory and regulatory milieu associated with Th17 and Treg cells. A) Comparing intestinal fatty acid binding protein (iFABP) concentration between HIV-unexposed uninfected infants (iHUU) and HIV-exposed uninfected infants (iHEU). B) Chemokine and cytokine concentrations in iHUU and iHEU at birth and 36 weeks. C) Cluster image map showing RV correlation of CD4 clusters with iFABP, chemokine and cytokine concentrations. D) Sparse PLS discriminant analysis (sPLS-DA) between HUU and HEU using CD4 clusters and chemokine data set E) ROC-curve analysis of LV-1 loadings at birth. F) Cluster image map of CD4 clusters and iFABP, chemokine and cytokine concentrations. G) sPLS-DA H) ROC-curve analysis of LV-1 loadings at week 36.